



Study of the rare B_s^0 and B^0 decays into the $\pi^+\pi^-\mu^+\mu^-$ final state



LHCb Collaboration

ARTICLE INFO

Article history:

Received 19 December 2014
 Received in revised form 3 February 2015
 Accepted 5 February 2015
 Available online 11 February 2015
 Editor: W.-D. Schlatter

ABSTRACT

A search for the rare decays $B_s^0 \rightarrow \pi^+\pi^-\mu^+\mu^-$ and $B^0 \rightarrow \pi^+\pi^-\mu^+\mu^-$ is performed in a data set corresponding to an integrated luminosity of 3.0 fb^{-1} collected by the LHCb detector in proton–proton collisions at centre-of-mass energies of 7 and 8 TeV. Decay candidates with pion pairs that have invariant mass in the range $0.5\text{--}1.3 \text{ GeV}/c^2$ and with muon pairs that do not originate from a resonance are considered. The first observation of the decay $B_s^0 \rightarrow \pi^+\pi^-\mu^+\mu^-$ and the first evidence of the decay $B^0 \rightarrow \pi^+\pi^-\mu^+\mu^-$ are obtained and the branching fractions, restricted to the dipion-mass range considered, are measured to be $\mathcal{B}(B_s^0 \rightarrow \pi^+\pi^-\mu^+\mu^-) = (8.6 \pm 1.5 \text{ (stat)} \pm 0.7 \text{ (syst)} \pm 0.7 \text{ (norm)}) \times 10^{-8}$ and $\mathcal{B}(B^0 \rightarrow \pi^+\pi^-\mu^+\mu^-) = (2.11 \pm 0.51 \text{ (stat)} \pm 0.15 \text{ (syst)} \pm 0.16 \text{ (norm)}) \times 10^{-8}$, where the third uncertainty is due to the branching fraction of the decay $B^0 \rightarrow J/\psi(\rightarrow \mu^+\mu^-)K^*(892)^0(\rightarrow K^+\pi^-)$, used as a normalisation.

© 2015 The Authors. Published by Elsevier B.V. This is an open access article under the CC BY license (<http://creativecommons.org/licenses/by/4.0/>). Funded by SCOAP³.

1. Introduction

Decays of the B_s^0 and B^0 mesons into a $\pi^+\pi^-\mu^+\mu^-$ final state with the muons not originating from a resonance are flavour-changing neutral-current transitions,¹ which are expected to proceed mainly from the $B_s^0 \rightarrow f_0(980)(\rightarrow \pi^+\pi^-)\mu^+\mu^-$ and $B^0 \rightarrow \rho(770)^0(\rightarrow \pi^+\pi^-)\mu^+\mu^-$ decays, in analogy to what is observed in $B_{(s)}^0 \rightarrow J/\psi\pi^+\pi^-$ decays [1,2]. In the standard model (SM) these decays are governed by the $b \rightarrow s$ and $b \rightarrow d$ weak transitions and are described by loop diagrams. They are suppressed due to the Glashow–Iliopoulos–Maiani mechanism [3] and the small values of the Cabibbo–Kobayashi–Maskawa matrix elements involved [4,5]. This feature makes the $B_s^0 \rightarrow f_0(980)\mu^+\mu^-$ and $B^0 \rightarrow \rho(770)^0\mu^+\mu^-$ decays sensitive probes of several SM extensions, since potential non-SM amplitudes may dominate over the SM contribution [6–10]. Current SM predictions of the $B_s^0 \rightarrow f_0(980)\mu^+\mu^-$ branching fraction vary from 10^{-7} to 10^{-9} [11–13]; similar values are expected for the $B^0 \rightarrow \rho(770)^0\mu^+\mu^-$ branching fraction [14–16]. The predictions suffer from uncertainties in the calculation of the hadronic matrix elements associated with the transitions. For the $B_s^0 \rightarrow f_0(980)\mu^+\mu^-$ decay, the limited knowledge of the quark content of the $f_0(980)$ meson results in additional uncertainties. No experimental information exists on these decays to date.

In this Letter, a search for the $B_{(s)}^0 \rightarrow \pi^+\pi^-\mu^+\mu^-$ decays is reported. The analysis is restricted to events with muons that do not originate from ϕ , J/ψ , and $\psi(2S)$ resonances, and with pion pairs with invariant mass in the range $0.5\text{--}1.3 \text{ GeV}/c^2$. This mass range is set to include both $f_0(980)$ and $\rho(770)^0$ resonances, which overlap because of their large widths [17]. Other resonances, as well as non-resonant pions, might contribute [1,2]. However, due to the limited size of the data sample, an amplitude analysis of the $\pi^+\pi^-$ mass spectrum is not attempted. The analysis is performed in a data set corresponding to an integrated luminosity of 3.0 fb^{-1} , collected by the LHCb detector in proton–proton (pp) collisions. The first 1.0 fb^{-1} of data was collected in 2011 with collisions at the centre-of-mass energy of 7 TeV; the remaining 2.0 fb^{-1} in 2012 at 8 TeV. The signal yields are obtained from a fit to the unbinned $\pi^+\pi^-\mu^+\mu^-$ mass distribution of the decay candidates. The fit modelling and the methods for the background estimation are validated on data, by fitting the $\pi^+\pi^-\mu^+\mu^-$ mass distribution of $B_{(s)}^0 \rightarrow J/\psi\pi^+\pi^-$ decays, while the branching fractions of $B_{(s)}^0 \rightarrow \pi^+\pi^-\mu^+\mu^-$ decays are normalised using $B^0 \rightarrow J/\psi K^*(892)^0$ decays reconstructed in the same data set.

2. Detector and simulation

The LHCb detector [18] is a single-arm forward spectrometer covering the pseudorapidity range $2 < \eta < 5$, designed for the study of particles containing b or c quarks. The detector includes a high-precision tracking system consisting of a silicon-strip vertex

¹ The inclusion of charge-conjugate processes is implied throughout.

detector surrounding the pp interaction region [19], a large-area silicon-strip detector located upstream of a dipole magnet with a bending power of about 4 Tm, and three stations of silicon-strip detectors and straw drift tubes [20] placed downstream of the magnet. The tracking system provides a measurement of momentum with a relative uncertainty that varies from 0.4% at low momentum to 0.6% at 100 GeV/c. The minimum distance of a track to a primary vertex (PV), the impact parameter (IP), is measured with a resolution of 20 μm for charged particles with high transverse momentum (p_T). Different types of charged hadrons are distinguished using information from two ring-imaging Cherenkov detectors (RICH) [21]. Photon, electron and hadron candidates are identified by a calorimeter system consisting of scintillating-pad and preshower detectors, an electromagnetic calorimeter and a hadronic calorimeter. Muons are identified by a system composed of alternating layers of iron and multiwire proportional chambers [22].

Samples of simulated events are used to determine the efficiency of selecting $B_{(s)}^0 \rightarrow \pi^+\pi^-\mu^+\mu^-$ and $B^0 \rightarrow J/\psi K^*(892)^0$ decays, and to study backgrounds. In the simulation, pp collisions are generated using PYTHIA [23,24] with a specific LHCb configuration [25]. Decays of hadronic particles are described by EVTGEN [26], in which final-state radiation is generated using PHOTOS [27]. The model of Refs. [12,28,29] is used to describe $B_{(s)}^0 \rightarrow \pi^+\pi^-\mu^+\mu^-$ decays. The interaction of the generated particles with the detector and its response are implemented using the GEANT4 toolkit [30,31] as described in Ref. [32].

3. Event selection

The online event-selection (trigger) consists of a hardware stage, based on information from the calorimeter and muon systems, followed by a software stage, which applies a full event reconstruction [33]. For this analysis, the hardware trigger requires at least one muon with $p_T > 1.48$ (1.76) GeV/c, or two muons with $\sqrt{p_T(\mu_1)p_T(\mu_2)} > 1.3$ (1.6) GeV/c, in the 2011 (2012) data sample. In the software trigger, at least one of the final-state particles is required to have $p_T > 1$ GeV/c and IP > 100 μm with respect to all the primary pp interaction vertices in the event. Finally, the tracks of two or more final-state particles are required to form a vertex that is significantly displaced from the PVs. A multivariate algorithm is used to identify secondary vertices consistent with the decay of a b hadron [34].

In the offline selection, all charged particles are required to have $p_T > 0.25$ GeV/c and trajectories not consistent with originating from the PVs. Two oppositely charged muon candidates compatible with originating from the same displaced vertex are considered. To reject $\phi \rightarrow \mu^+\mu^-$, $J/\psi \rightarrow \mu^+\mu^-$, and $\psi(2S) \rightarrow \mu^+\mu^-$ decays, candidates having invariant mass in the ranges 1.010–1.030, 2.796–3.216, or 3.436–3.806 GeV/ c^2 are removed; contributions from other resonances in the $\mu^+\mu^-$ mass spectrum such as $\rho(770)^0$, $\omega(782)$, and $\psi(4160)$ [35] are negligible. The muon candidates are combined with a pair of oppositely charged pions with invariant mass in the range 0.5–1.3 GeV/ c^2 to form $B_{(s)}^0 \rightarrow \pi^+\pi^-\mu^+\mu^-$ candidates. For the $B^0 \rightarrow J/\psi(\rightarrow \mu^+\mu^-)K^*(892)^0(\rightarrow K^+\pi^-)$ candidates, the dimuon invariant mass is required to be in the range 2.796–3.216 GeV/ c^2 , and the invariant mass of the pion and kaon system in the range 0.826–0.966 GeV/ c^2 . The four tracks are required to originate from the same $B_{(s)}^0$ decay vertex. The $B_{(s)}^0$ momentum vector is required to be within 14 mrad of the vector that joins the PV with the $B_{(s)}^0$ decay vertex (flight distance vector).

The information from the RICH, the calorimeters, and the muon systems is used for particle identification (PID), i.e., to define a

likelihood for each track to be associated with a certain particle hypothesis. Requirements on the muon-identification likelihood are applied to reduce to $\mathcal{O}(10^{-2})$ the rate of misidentified muon candidates, mainly pions, whilst preserving 95% signal efficiency. In the case of $B^0 \rightarrow J/\psi K^*(892)^0$ decays, PID requirements on kaon candidates are applied to suppress any contributions from $B_{(s)}^0 \rightarrow J/\psi \pi^+\pi^-$ decays with pions misidentified as kaons. In the case of $B_{(s)}^0 \rightarrow \pi^+\pi^-\mu^+\mu^-$ decays, a requirement on the PID of pion candidates is applied to reduce the contamination from $B^0 \rightarrow K^*(892)^0(\rightarrow K^+\pi^-)\mu^+\mu^-$ decays with kaons misidentified as pions; this background peaks around 5.25 GeV/ c^2 in the $\pi^+\pi^-\mu^+\mu^-$ mass spectrum. A large data set of $B^0 \rightarrow J/\psi \pi^+\pi^-$ decays is used to optimise the PID requirement of pion candidates, assuming that the proportion between misidentified $B^0 \rightarrow J/\psi K^*(892)^0$ and $B^0 \rightarrow J/\psi \pi^+\pi^-$ decays is similar to the proportion between misidentified $B^0 \rightarrow K^*(892)^0\mu^+\mu^-$ and $B^0 \rightarrow \pi^+\pi^-\mu^+\mu^-$ decays. The requirement retains about 55% of the signal candidates. Simulations show that additional contributions from $B_s^0 \rightarrow \phi(\rightarrow K^+K^-)\mu^+\mu^-$ decays with double kaon-pion misidentification are negligible. A requirement on the proton-identification likelihood of pion candidates suppresses the contamination from decays with protons misidentified as pions, with a 95% signal efficiency. After this selection, simulations show that contributions from $\Lambda_b^0 \rightarrow \Lambda(\rightarrow p\pi^-)\mu^+\mu^-$ and $\Lambda_b^0 \rightarrow p\pi^-\mu^+\mu^-$ decays are negligible, as are contributions from $\Lambda_b^0 \rightarrow \Lambda(1520)(\rightarrow pK^-)\mu^+\mu^-$ and $\Lambda_b^0 \rightarrow pK^-\mu^+\mu^-$ decays, where both the proton and the kaon are misidentified as pions.

In addition to the above requirements, a multivariate selection based on a boosted decision tree (BDT) [36,37] is used to suppress the large background from random combinations of tracks (combinatorial background) present in the $\pi^+\pi^-\mu^+\mu^-$ sample. The BDT is trained using simulated $B_s^0 \rightarrow \pi^+\pi^-\mu^+\mu^-$ events to model the signal, and data candidates with $\pi^+\pi^-\mu^+\mu^-$ mass in the range 5.5–5.8 GeV/ c^2 for the background. The training is performed separately for the 2011 and 2012 data, and using simulations that reproduce the specific operational conditions of each year. The variables used in the BDT are the significance of the displacement from the PV of pion and muon tracks, the fit χ^2 of the $B_{(s)}^0$ decay vertex, the angle between the $B_{(s)}^0$ momentum vector and the flight distance vector, the p_T of the $B_{(s)}^0$ candidate, the sum and the difference of the transverse momenta of pions, the difference of the transverse momenta of muons, the $B_{(s)}^0$ decay time, and the minimum p_T of the pions. The resulting BDT output is independent of the $\pi^+\pi^-\mu^+\mu^-$ mass and PID variables. A requirement on the BDT output value is chosen to maximise the figure of merit $\varepsilon/(\alpha/2 + \sqrt{N_b})$ [38], where ε is the signal efficiency; N_b is the number of background events that pass the selection and have a mass within 30 MeV/ c^2 of the known value of the B_s^0 mass [17]; α represents the desired significance of the signal, expressed in terms of number of standard deviations. The value of α is set to 3 (5) for the 2011 (2012) data set. The resulting selection has around 85% efficiency to select signal candidates. The same BDT is used to select $B^0 \rightarrow J/\psi K^*(892)^0$ candidates. The selected samples consist of 364 $B_{(s)}^0 \rightarrow \pi^+\pi^-\mu^+\mu^-$ candidates and 52960 $B^0 \rightarrow J/\psi K^*(892)^0$ candidates.

The efficiencies of all selection requirements are estimated with simulations, except for the efficiency of the PID selection for hadrons. The latter is determined in data using large and low-background samples of $D^{*+} \rightarrow D^0(\rightarrow K^-\pi^+)\pi^+$ decays; the efficiencies are evaluated after reweighting the calibration samples to match simultaneously the momentum and pseudorapidity distributions of the final-state particles of $B_{(s)}^0 \rightarrow \pi^+\pi^-\mu^+\mu^-$

Table 1

Selection efficiencies of the 2011 and 2012 data sets; ε_s for the $B_s^0 \rightarrow \pi^+\pi^-\mu^+\mu^-$ decay, ε_d for the $B^0 \rightarrow \pi^+\pi^-\mu^+\mu^-$ decay, and ε_n for the $B^0 \rightarrow J/\psi K^*(892)^0$ decay.

| | 2011 | 2012 |
|---------------------|--|--|
| ε_s [%] | 36.1 ± 0.3 (stat) ± 2.4 (syst) | 36.9 ± 0.3 (stat) ± 2.3 (syst) |
| ε_d [%] | 29.8 ± 0.2 (stat) ± 2.0 (syst) | 27.5 ± 0.2 (stat) ± 1.7 (syst) |
| ε_n [%] | 9.33 ± 0.05 (stat) ± 0.35 (syst) | 9.74 ± 0.08 (stat) ± 0.27 (syst) |

($B^0 \rightarrow J/\psi K^*(892)^0$) candidates, and the distribution of the track multiplicity of the events. The final selection efficiencies for 2011 and 2012 data are reported in Table 1. The statistical uncertainties are due to the size of the calibration and simulation samples; systematic uncertainties are described in what follows. The total efficiency varies by approximately 15% in the $\pi^+\pi^-$ mass range considered and it is parametrised with a second-order polynomial. The signal candidates are weighted in order to have a constant efficiency as a function of the $\pi^+\pi^-$ mass spectrum.

Systematic uncertainties of the efficiencies are dominated by the limited information about the signal decay-models; the main contribution comes from the unknown angular distributions of $B_{(s)}^0 \rightarrow \pi^+\pi^-\mu^+\mu^-$ decay products. To estimate this uncertainty, the difference in efficiencies between decays generated according to a phase-space model and to the model of Refs. [12,28,29] is considered. The resulting relative uncertainty is 5.4%. A relative uncertainty of 3.7% (2.8%) for 2011 (2012) data is estimated by considering the difference of the efficiencies evaluated in the simulation and in data for $B^0 \rightarrow J/\psi K^*(892)^0$ decays. The same relative uncertainty is assigned to the efficiency associated with $B_{(s)}^0 \rightarrow \pi^+\pi^-\mu^+\mu^-$ decays, as the cancellation of this uncertainty in the ratio of the efficiencies of signal and normalisation decays may not be exact. This is due to the fact that the p_T distributions of the final-state particles are different between the decay modes. An additional 1.6% relative uncertainty is assigned to ε_s , due to the unknown mixture of B_s^0 mass eigenstates in $B_s^0 \rightarrow \pi^+\pi^-\mu^+\mu^-$ decays, which results in a B_s^0 effective lifetime that could differ from the value used in the simulations [39].

4. Determination of the signal yields

The ratio of the branching fractions

$$\mathcal{R}_q \equiv \frac{\mathcal{B}(B_{(s)}^0 \rightarrow \pi^+\pi^-\mu^+\mu^-)}{\mathcal{B}(B^0 \rightarrow J/\psi(\rightarrow \mu^+\mu^-)K^*(892)^0(\rightarrow K^+\pi^-))},$$

with $q = s$ (d) for $B_s^0 \rightarrow \pi^+\pi^-\mu^+\mu^-$ ($B^0 \rightarrow \pi^+\pi^-\mu^+\mu^-$) decays, is the quantity being measured; it is used to express the observed yields of $B_{(s)}^0 \rightarrow \pi^+\pi^-\mu^+\mu^-$ decays as follows:

$$N_{B_q} = \frac{f_q \varepsilon_q}{f_d \varepsilon_n} N_n \mathcal{R}_q, \quad (1)$$

where N_n is the $B^0 \rightarrow J/\psi K^*(892)^0$ yield, f_s/f_d is the ratio of the fragmentation probabilities for B_s^0 and B^0 mesons [40], ε_q is the selection efficiency of $B_s^0 \rightarrow \pi^+\pi^-\mu^+\mu^-$ ($B^0 \rightarrow \pi^+\pi^-\mu^+\mu^-$) decays, and ε_n is the one of $B^0 \rightarrow J/\psi K^*(892)^0$ decays.

The number of events N_n in Eq. (1) is obtained from an extended maximum likelihood fit to the unbinned $\mu^+\mu^-K^+\pi^-$ mass distribution of the $B^0 \rightarrow J/\psi K^*(892)^0$ candidates in the range 4.97–5.77 GeV/ c^2 . The $\mu^+\mu^-K^+\pi^-$ mass distribution is shown in Fig. 1 with fit projections overlaid. A sum of two Gaussian functions, with a power-law tail on either side derived from simulations, is used to describe the dominant $B^0 \rightarrow J/\psi K^*(892)^0$ peak and the small $B_s^0 \rightarrow J/\psi K^*(892)^0$ contribution. All function

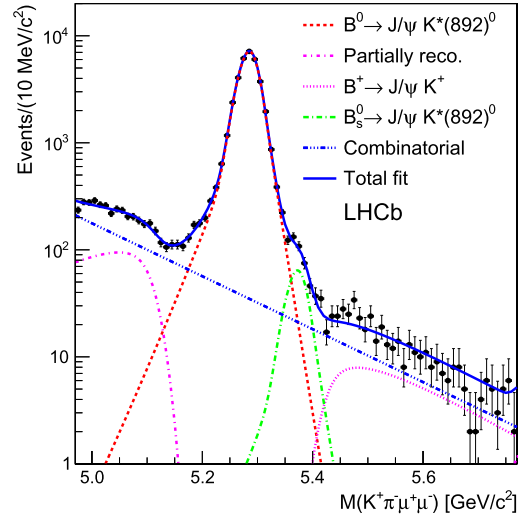


Fig. 1. Mass distribution of $B^0 \rightarrow J/\psi K^*(892)^0$ candidates with fit projections overlaid. The 2011 and 2012 data sets are combined.

parameters are in common between the B^0 and B_s^0 signal functions, except for the mass; the mass difference between B_s^0 and B^0 mesons is fixed to the known value [17]. An exponential function is used to model the combinatorial background. A small contamination of $B^+ \rightarrow J/\psi K^+$ decays combined with an additional charged pion is modelled with an ARGUS function [41]. Partially reconstructed B^0 decays at masses lower than the B^0 signal are described with another ARGUS function. The fitted yields of $B^0 \rightarrow J/\psi K^*(892)^0$ decays are corrected by subtracting a $(6.4 \pm 1.0)\%$ contribution of $B^0 \rightarrow J/\psi K^+\pi^-$ decays [42], where the $K^+\pi^-$ pair is in a S -wave state and does not originate from the decay of a $K^*(892)^0$ resonance. The numbers of $B^0 \rightarrow J/\psi K^*(892)^0$ decays are 9821 ± 110 (stat) ± 134 (syst) ± 97 (S wave) and 23521 ± 175 (stat) ± 172 (syst) ± 243 (S wave) in the 2011 and 2012 data sets, respectively, where the third uncertainty is due to the S -wave subtraction. The systematic uncertainty accounts for the uncertainties in the parameters fixed in the fit to the values determined in simulations, and are calculated with the method described at the end of this section.

The ratios \mathcal{R}_s and \mathcal{R}_d are measured from an extended maximum likelihood fit to the unbinned $\pi^+\pi^-\mu^+\mu^-$ mass distribution, where the signal yields are parametrised using Eq. (1), and all other inputs are fixed. The different centre-of-mass energies result in different $b\bar{b}$ production cross sections and selection efficiencies in the 2011 and 2012 data samples. Therefore, the two samples are fitted simultaneously with different likelihood functions, but with the parameters \mathcal{R}_s and \mathcal{R}_d in common. We also fit simultaneously the $B_{(s)}^0 \rightarrow \pi^+\pi^-\mu^+\mu^-$ and $B_{(s)}^0 \rightarrow J/\psi \pi^+\pi^-$ samples. The latter are selected with the $B_{(s)}^0 \rightarrow \pi^+\pi^-\mu^+\mu^-$ requirements, except for the dimuon mass, which is restricted to the 2.796–3.216 GeV/ c^2 range. The $B_{(s)}^0 \rightarrow J/\psi \pi^+\pi^-$ fit serves as a consistency check of the fit modelling, since the $B_{(s)}^0 \rightarrow \pi^+\pi^-\mu^+\mu^-$ and $B_{(s)}^0 \rightarrow J/\psi \pi^+\pi^-$ mass distributions are expected to be similar. In both samples, the fit range is 2 GeV/ c^2 wide and starts from 5.19 GeV/ c^2 . This limit is set to remove partially reconstructed decays of the B^0 mesons with an unreconstructed π^0 . The stability of the fit results is checked against the extension of the fit range in the lower mass region of the $B_{(s)}^0 \rightarrow \pi^+\pi^-\mu^+\mu^-$ and $B_{(s)}^0 \rightarrow J/\psi \pi^+\pi^-$ mass distributions, where an additional component is needed in the fit to describe the partially reconstructed B^0 decays below 5.19 GeV/ c^2 .

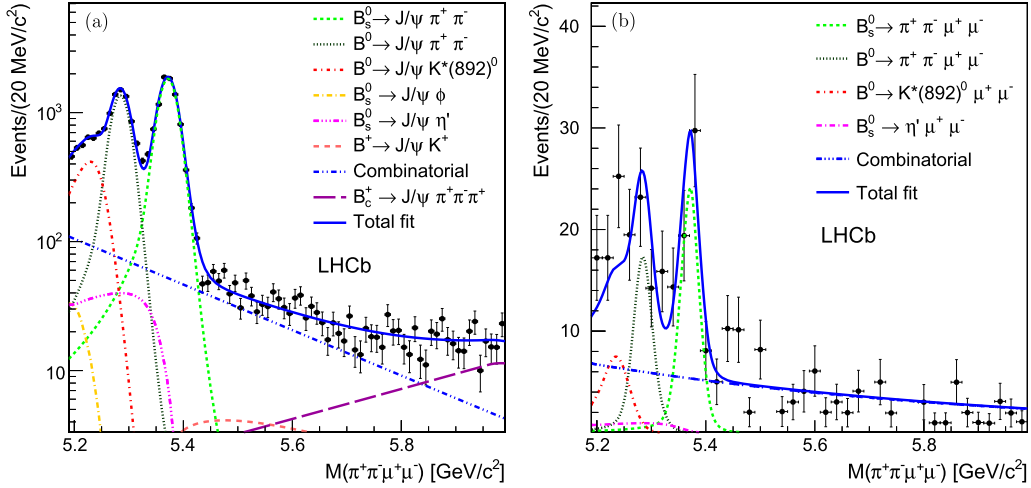


Fig. 2. Mass distributions of (a) the $B_{(s)}^0 \rightarrow J/\psi \pi^+ \pi^-$ and (b) the $B_{(s)}^0 \rightarrow \pi^+ \pi^- \mu^+ \mu^-$ decay candidates in the range 5.19–5.99 GeV/c^2 with fit projections overlaid. The 2011 and 2012 data sets are combined. In (b), the contribution from $B_s^0 \rightarrow \phi \mu^+ \mu^-$ and $B^+ \rightarrow K^+ \mu^+ \mu^-$ decays are included in the fit, but they are not visible in the projection, because the corresponding yields are small.

Fig. 2 shows the $\pi^+ \pi^- \mu^+ \mu^-$ mass distributions of the $B_{(s)}^0 \rightarrow J/\psi \pi^+ \pi^-$ and $B_{(s)}^0 \rightarrow \pi^+ \pi^- \mu^+ \mu^-$ decay candidates in the range 5.19–5.99 GeV/c^2 with fit projections overlaid, where the 2011 and 2012 data sets are combined.

The $B_{(s)}^0 \rightarrow \pi^+ \pi^- \mu^+ \mu^-$ and $B_{(s)}^0 \rightarrow J/\psi \pi^+ \pi^-$ signals are described by a model similar to that used for the $B^0 \rightarrow J/\psi K^*(892)^0$ signal in the fit of the $\mu^+ \mu^- K^+ \pi^-$ mass distribution. The B^0 peak position is a common parameter for the $B_{(s)}^0 \rightarrow \pi^+ \pi^- \mu^+ \mu^-$ and $B_{(s)}^0 \rightarrow J/\psi \pi^+ \pi^-$ fits, as well as the signal resolutions; the difference between the B^0 and the B_s^0 masses is fixed to the known value. The $B_{(s)}^0 \rightarrow \pi^+ \pi^- \mu^+ \mu^-$ signal widths are multiplied by scale factors, derived from simulations, which accounts for the different momentum spectra between non-resonant muons and muons from J/ψ meson decays. In both fits, the combinatorial background is modelled with an exponential function.

Backgrounds from $B^0 \rightarrow K^*(892)^0 \mu^+ \mu^-$ ($B^0 \rightarrow J/\psi K^*(892)^0$) decays, where kaons are misidentified as pions, are estimated using control samples of these decays reconstructed in data. They are selected as $B_{(s)}^0 \rightarrow \pi^+ \pi^- \mu^+ \mu^-$ ($B_{(s)}^0 \rightarrow J/\psi \pi^+ \pi^-$) candidates, except for different requirements on the PID variables of the kaon and pion candidates, as for the normalisation decay mode. To obtain the yields and the shapes of the mass distribution of the misidentified decays, the kaon candidates are assigned the pion mass, and the resulting $\pi^+ \pi^- \mu^+ \mu^-$ mass distribution is reweighted to reproduce the PID selection of the $B_{(s)}^0 \rightarrow \pi^+ \pi^- \mu^+ \mu^-$ sample. In the final fit, the yields of the two backgrounds are constrained using Gaussian functions with means fixed to the values obtained with this method, and widths that account for a relative uncertainty in the 2011 (2012) data sample of 15% (10%) for $B^0 \rightarrow K^*(892)^0 \mu^+ \mu^-$ decays, and of 2% (1%) for $B^0 \rightarrow J/\psi K^*(892)^0$ decays. The shape of the $B^0 \rightarrow K^*(892)^0 \mu^+ \mu^-$ background is modelled with a Gaussian function with a power-law tail on the low-mass side; the shape of the $B^0 \rightarrow J/\psi K^*(892)^0$ background is modelled with a sum of two Gaussian functions with different means. All parameters of these functions are fixed from the values obtained in the fit to the control samples. The background from $B_s^0 \rightarrow J/\psi K^*(892)^0$ decays is expected to be less than 0.5% [17] of the $B^0 \rightarrow J/\psi K^*(892)^0$ yield and is neglected. Similarly, the background from $B_s^0 \rightarrow K^*(892)^0 \mu^+ \mu^-$ decays is not considered.

Table 2

Summary of systematic uncertainties on \mathcal{R}_s and \mathcal{R}_d .

| Source | $\sigma(\mathcal{R}_s)$ [10^{-3}] | $\sigma(\mathcal{R}_d)$ [10^{-3}] |
|--------------------------------|---------------------------------------|---------------------------------------|
| Shape of misidentified decays | 0.003 | 0.004 |
| Partially reconstructed decays | 0.003 | 0.004 |
| Combinatorial background | 0.029 | 0.014 |
| Signal shapes | 0.020 | 0.014 |
| Efficiencies | 0.061 | 0.013 |
| Normalisation decay yields | 0.055 | 0.014 |
| f_s/f_d | 0.093 | – |
| Quadratic sum | 0.130 | 0.028 |

Backgrounds from decays $B_s^0 \rightarrow \phi(\rightarrow \pi^+ \pi^- \pi^0) \mu^+ \mu^-$ with an unreconstructed π^0 , $B_s^0 \rightarrow \eta'(\rightarrow \pi^+ \pi^- \gamma) \mu^+ \mu^-$ with an unreconstructed γ , and $B^+ \rightarrow K^+ \mu^+ \mu^-$ or $B^+ \rightarrow \pi^+ \mu^+ \mu^-$ combined with an additional charged pion, are estimated from simulations. The mass distributions of these backgrounds are modelled with ARGUS functions with parameters fixed from fits to simulated events. Backgrounds from similar decay modes, where the muons come from the J/ψ meson, are described in the $B_{(s)}^0 \rightarrow J/\psi \pi^+ \pi^-$ fit using the same methods. An additional contribution is given by $B_c^+ \rightarrow J/\psi \pi^+ \pi^- \pi^+$ decays, where a pion is not reconstructed. This background is modelled with a sum of two Gaussian functions, one of which has a power-law tail on the low-mass side. Backgrounds from semileptonic $B^0 \rightarrow D^-(\rightarrow \rho^0 \mu^- X) \mu^+ X$ decays with $\rho^0 \rightarrow \pi^+ \pi^-$, give a negligible contribution at $\pi^+ \pi^- \mu^+ \mu^-$ mass greater than 5.19 GeV/c^2 .

5. Results

We measure $\mathcal{R}_s = (1.67 \pm 0.29 \text{ (stat)} \pm 0.13 \text{ (syst)}) \times 10^{-3}$ and $\mathcal{R}_d = (0.41 \pm 0.10 \text{ (stat)} \pm 0.03 \text{ (syst)}) \times 10^{-3}$. Systematic uncertainties are discussed below. These values correspond to $55 \pm 10 \text{ (stat)} \pm 5 \text{ (syst)}$ $B_s^0 \rightarrow \pi^+ \pi^- \mu^+ \mu^-$ decays and $40 \pm 10 \text{ (stat)} \pm 3 \text{ (syst)}$ $B^0 \rightarrow \pi^+ \pi^- \mu^+ \mu^-$ decays. The significances of the observed signals are calculated using Wilks' theorem [43], and are 7.2σ and 4.8σ for the $B_s^0 \rightarrow \pi^+ \pi^- \mu^+ \mu^-$ and $B^0 \rightarrow \pi^+ \pi^- \mu^+ \mu^-$ decays, respectively. The $B_s^0 \rightarrow \pi^+ \pi^- \mu^+ \mu^-$ ($B^0 \rightarrow \pi^+ \pi^- \mu^+ \mu^-$) significance is obtained by considering the $B^0 \rightarrow \pi^+ \pi^- \mu^+ \mu^-$ ($B_s^0 \rightarrow \pi^+ \pi^- \mu^+ \mu^-$) yield as a floating parameter in the fit. The systematic uncertainties are included by multiplying the signif-

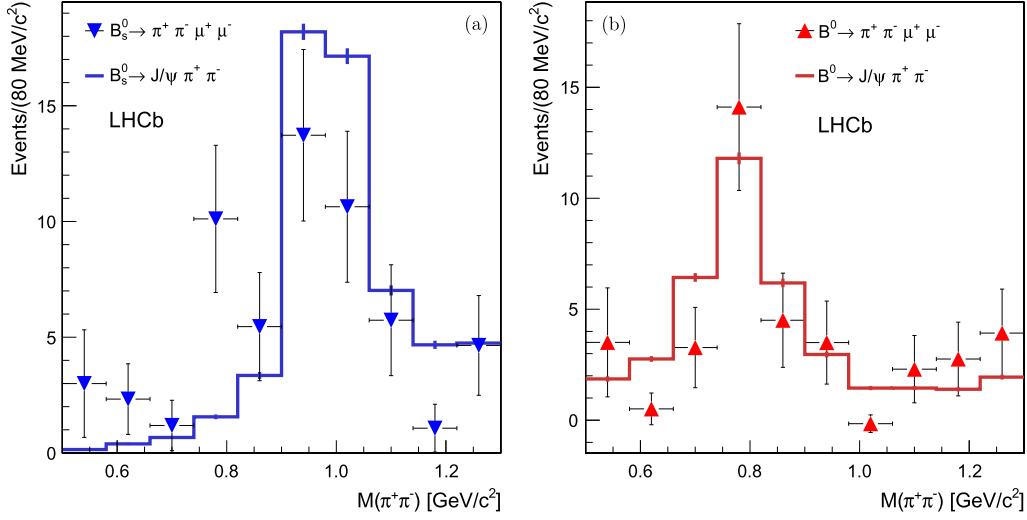


Fig. 3. Background-subtracted distributions of the $\pi^+\pi^-$ invariant mass for (a) $B_s^0 \rightarrow \pi^+\pi^-\mu^+\mu^-$ and (b) $B^0 \rightarrow \pi^+\pi^-\mu^+\mu^-$ candidates (triangular markers). The uncertainties are statistical only. The data are compared with the background-subtracted $\pi^+\pi^-$ mass distributions of (a) $B_s^0 \rightarrow J/\psi\pi^+\pi^-$ and (b) $B^0 \rightarrow J/\psi\pi^+\pi^-$ candidates (histograms).

icance by the factor $1/\sqrt{1 + (\sigma_{\text{stat}}/\sigma_{\text{stat}})^2}$, where σ_{stat} is the statistical uncertainty, and σ_{syst} is the sum in quadrature of the contributions in Table 2, except for the uncertainty on f_s/f_d .

Fig. 3 compares the $\pi^+\pi^-$ mass spectra of $B_{(s)}^0 \rightarrow \pi^+\pi^-\mu^+\mu^-$ and $B_{(s)}^0 \rightarrow J/\psi\pi^+\pi^-$ candidates, separately for the B_s^0 and the B^0 decays. The background is subtracted using the *sPlot* technique [44] with the $\pi^+\pi^-\mu^+\mu^-$ mass as the discriminating variable. The data show the dominance of the $f_0(980)$ resonance in the case of $B_s^0 \rightarrow J/\psi\pi^+\pi^-$ decays, and of the $\rho(770)^0$ resonance in the case of $B^0 \rightarrow J/\psi\pi^+\pi^-$ decays, as expected from previous LHCb analyses [1,2]. The $B_{(s)}^0 \rightarrow \pi^+\pi^-\mu^+\mu^-$ data show indications of a similar composition of the $\pi^+\pi^-$ mass spectrum, although the size of the sample is not sufficient to draw a definite conclusion.

Several systematic uncertainties on \mathcal{R}_s and \mathcal{R}_d are considered, as summarised in Table 2. The contribution due to the uncertainties on parameters that are fixed in the fit, and on the efficiencies and the yields of $B^0 \rightarrow J/\psi K^*(892)^0$ decays that are fixed in Eq. (1), is obtained by repeating the fit, each time with the relevant parameters or inputs fixed to alternate values. These are sampled from Gaussian distributions centred at the nominal value, and whose widths correspond to the uncertainties on the fixed parameters and inputs. Known correlations between fixed parameters are taken into account. The r.m.s. spreads of the resulting \mathcal{R}_s and \mathcal{R}_d values are taken as the systematic uncertainties. The uncertainties associated with efficiencies are the sums in quadrature of their statistical and systematic uncertainties, reported in Table 1. The uncertainty on the $B^0 \rightarrow J/\psi K^*(892)^0$ yield is the sum in quadrature of the statistical uncertainty, the systematic uncertainty, and the uncertainty due to the *S*-wave subtraction. A systematic uncertainty is assigned on the estimation of the combinatorial background with the following method; pseudo experiments are generated in an extended mass range from $4.97 \text{ GeV}/c^2$, where an additional peaking component is also added to simulate the partially reconstructed B^0 decays, and the pseudo data are fitted in the nominal range from $5.19 \text{ GeV}/c^2$. The shifts between the average fitted values and the input values of \mathcal{R}_s and \mathcal{R}_d are taken as the systematic uncertainties. The contribution to the systematic uncertainty of \mathcal{R}_s due to the uncertainty on the values of f_s/f_d is also included. The final systematic uncertainties

are the sums in quadrature of all contributions and correspond to 45% and 28% of the statistical uncertainties of \mathcal{R}_s and \mathcal{R}_d , respectively.

6. Conclusions

The first observation of the decay $B_s^0 \rightarrow \pi^+\pi^-\mu^+\mu^-$ and the first evidence of the decay $B^0 \rightarrow \pi^+\pi^-\mu^+\mu^-$ are obtained in a data set corresponding to an integrated luminosity of 3.0 fb^{-1} collected by the LHCb detector in *pp* collisions at centre-of-mass energies of 7 and 8 TeV. The analysis is restricted to candidates with muon pairs that do not originate from ϕ , J/ψ , and $\psi(2S)$ resonances, while the pion pairs are required to have invariant mass in the range $0.5\text{--}1.3 \text{ GeV}/c^2$. About 55 $B_s^0 \rightarrow \pi^+\pi^-\mu^+\mu^-$ decays and 40 $B^0 \rightarrow \pi^+\pi^-\mu^+\mu^-$ decays are observed with significances of 7.2σ and 4.8σ , respectively. Their branching fractions relative to the branching fraction of the $B^0 \rightarrow J/\psi(\rightarrow \mu^+\mu^-)K^*(892)^0(\rightarrow K^+\pi^-)$ decay are measured to be

$$\frac{\mathcal{B}(B_s^0 \rightarrow \pi^+\pi^-\mu^+\mu^-)}{\mathcal{B}(B^0 \rightarrow J/\psi(\rightarrow \mu^+\mu^-)K^*(892)^0(\rightarrow K^+\pi^-))} = (1.67 \pm 0.29 \text{ (stat)} \pm 0.13 \text{ (syst)}) \times 10^{-3},$$

$$\frac{\mathcal{B}(B^0 \rightarrow \pi^+\pi^-\mu^+\mu^-)}{\mathcal{B}(B^0 \rightarrow J/\psi(\rightarrow \mu^+\mu^-)K^*(892)^0(\rightarrow K^+\pi^-))} = (0.41 \pm 0.10 \text{ (stat)} \pm 0.03 \text{ (syst)}) \times 10^{-3}.$$

From these ratios, the following branching fractions are obtained for the decays with the dipion-mass range considered:

$$\mathcal{B}(B_s^0 \rightarrow \pi^+\pi^-\mu^+\mu^-) = (8.6 \pm 1.5 \text{ (stat)} \pm 0.7 \text{ (syst)} \pm 0.7 \text{ (norm)}) \times 10^{-8} \text{ and}$$

$$\mathcal{B}(B^0 \rightarrow \pi^+\pi^-\mu^+\mu^-) = (2.11 \pm 0.51 \text{ (stat)} \pm 0.15 \text{ (syst)} \pm 0.16 \text{ (norm)}) \times 10^{-8},$$

where the third uncertainties are due to the uncertainties on the branching fraction of the normalisation decay. We use $\mathcal{B}(B^0 \rightarrow J/\psi K^*(892)^0) = (1.30 \pm 0.10) \times 10^{-3}$, which is the weighted average of measurements where the $K^+\pi^-$ *S*-wave contribution is subtracted [45–47], $\mathcal{B}(J/\psi \rightarrow \mu^+\mu^-)$ from Ref. [17], and $\mathcal{B}(K^*(892)^0 \rightarrow K^+\pi^-) = 2/3$.

Assuming that the decays $f_0(980) \rightarrow \pi^+\pi^-$ and $\rho(770)^0 \rightarrow \pi^+\pi^-$ are the dominant transitions in the $B_s^0 \rightarrow \pi^+\pi^-\mu^+\mu^-$ and $B^0 \rightarrow \pi^+\pi^-\mu^+\mu^-$ decays, respectively, and neglecting other contributions, the $B_{(s)}^0 \rightarrow \pi^+\pi^-\mu^+\mu^-$ branching fractions are corrected to account for the selection efficiencies of the $f_0(980)$ and $\rho(770)^0$ resonances in the $\pi^+\pi^-$ mass range considered. The following values are obtained: $\mathcal{B}(B_s^0 \rightarrow f_0(980)(\rightarrow \pi^+\pi^-)\mu^+\mu^-) = (8.3 \pm 1.7) \times 10^{-8}$ and $\mathcal{B}(B^0 \rightarrow \rho(770)^0\mu^+\mu^-) = (1.98 \pm 0.53) \times 10^{-8}$, where all uncertainties are summed in quadrature. These values favour SM expectations of Refs. [12,14,15] and disfavour the $\mathcal{B}(B_s^0 \rightarrow f_0(980)\mu^+\mu^-)$ SM expectation of Ref. [13].

Acknowledgements

We express our gratitude to our colleagues in the CERN accelerator departments for the excellent performance of the LHC. We thank the technical and administrative staff at the LHCb institutes. We acknowledge support from CERN and from the national agencies: CAPES, CNPq, FAPERJ and FINEP (Brazil); NSFC (China); CNRS/IN2P3 (France); BMBF, DFG, HGF and MPG (Germany); INFN (Italy); FOM and NWO (The Netherlands); MNiSW and NCN (Poland); MEN/IFA (Romania); MinES and FANO (Russia); MinEco (Spain); SNSF and SER (Switzerland); NASU (Ukraine); STFC (United Kingdom); NSF (USA). The Tier1 computing centres are supported by IN2P3 (France), KIT and BMBF (Germany), INFN (Italy), NWO and SURF (The Netherlands), PIC (Spain), GridPP (United Kingdom). We are indebted to the communities behind the multiple open source software packages on which we depend. We are also thankful for the computing resources and the access to software R&D tools provided by Yandex LLC (Russia). Individual groups or members have received support from EPLANET, Marie Skłodowska-Curie Actions and ERC (European Union), Conseil général de Haute-Savoie, Labex ENIGMASS and OCEVU, Région Auvergne (France), RFBR (Russia), XuntaGal and GENCAT (Spain), Royal Society and Royal Commission for the Exhibition of 1851 (United Kingdom).

References

- [1] LHCb Collaboration, R. Aaij, et al., Measurement of the resonant and CP components in $\bar{B}^0 \rightarrow J/\psi\pi^+\pi^-$ decays, Phys. Rev. D 90 (2014) 012003, arXiv:1404.5673.
- [2] LHCb Collaboration, R. Aaij, et al., Measurement of resonant and CP components in $\bar{B}_s^0 \rightarrow J/\psi\pi^+\pi^-$ decays, Phys. Rev. D 89 (2014) 092006, arXiv:1402.6248.
- [3] S.L. Glashow, J. Iliopoulos, L. Maiani, Weak interactions with lepton-hadron symmetry, Phys. Rev. D 2 (1970) 1285.
- [4] N. Cabibbo, Unitary symmetry and leptonic decays, Phys. Rev. Lett. 10 (1963) 531.
- [5] M. Kobayashi, T. Maskawa, CP-violation in the renormalizable theory of weak interaction, Prog. Theor. Phys. 49 (1973) 652.
- [6] R. Mohanta, Study of some B_s^0 to $f_0(980)$ decays in the fourth generation model, Phys. Rev. D 84 (2011) 014019, arXiv:1104.4739.
- [7] V. Bashiry, K. Azizi, Systematic analysis of the $B_s \rightarrow f_0\ell^+\ell^-$ in the universal extra dimension, J. High Energy Phys. 1202 (2012) 021, arXiv:1112.5243.
- [8] E. Ilhan, The exclusive $\bar{B} \rightarrow \pi e^+e^-$ and $\bar{B} \rightarrow \rho e^+e^-$ decays in the two Higgs doublet model with flavor changing neutral currents, Int. J. Mod. Phys. A 14 (1999) 4365, arXiv:hep-ph/9807256.
- [9] T. Aliev, M. Savci, Exclusive $B \rightarrow \pi^+l^+l^-$ and $B \rightarrow \rho^+l^+l^-$ decays in two Higgs doublet model, Phys. Rev. D 60 (1999) 014005, arXiv:hep-ph/9812272.
- [10] J.-J. Wang, R.-M. Wang, Y.-G. Xu, Y.-D. Yang, Rare decays $B^+ \rightarrow \pi^+l^+l^-$, $\rho^+l^+l^-$ and $B^0 \rightarrow l^+l^-$ in the R-parity violating supersymmetry, Phys. Rev. D 77 (2008) 014017, arXiv:0711.0321.
- [11] R.-H. Li, C.-D. Lu, W. Wang, X.-X. Wang, $b \rightarrow s$ transition form factors in the pQCD approach, Phys. Rev. D 79 (2009) 014013, arXiv:0811.2648.
- [12] P. Colangelo, F. De Fazio, W. Wang, $B_s \rightarrow f_0(980)$ form factors and B_s decays into $f_0(980)$, Phys. Rev. D 81 (2010) 074001, arXiv:1002.2880.
- [13] N. Ghahramany, R. Khosravi, Analysis of the rare semileptonic decays of B_s^0 to $f_0(980)$ and $K^*(1430)^0$ scalar mesons in QCD sum rules, Phys. Rev. D 80 (2009) 016009.
- [14] F. Kruger, L. Sehgal, CP violation in the exclusive decays $B \rightarrow \pi e^+e^-$ and $B \rightarrow \rho e^+e^-$, Phys. Rev. D 56 (1997) 5452, arXiv:hep-ph/9706247.
- [15] D. Melikhov, N.V. Nikitin, Form factors for rare decays $B \rightarrow (\pi, \rho, K, K^*)l^+l^-$ in the quark model, arXiv:hep-ph/9609503.
- [16] M. Beneke, T. Feldmann, D. Seidel, Exclusive radiative and electroweak $b \rightarrow d$ and $b \rightarrow s$ penguin decays at NLO, Eur. Phys. J. C 41 (2005) 173, arXiv:hep-ph/0412400.
- [17] Particle Data Group, K.A. Olive, et al., Review of particle physics, Chin. Phys. C 38 (2014) 090001.
- [18] LHCb Collaboration, A.A. Alves Jr., et al., The LHCb detector at the LHC, J. Instrum. 3 (2008) S08005.
- [19] R. Aaij, et al., Performance of the LHCb vertex locator, J. Instrum. 9 (2014) P09007, arXiv:1405.7808.
- [20] R. Arink, et al., Performance of the LHCb outer tracker, J. Instrum. 9 (2014) P01002, arXiv:1311.3893.
- [21] M. Adinolfi, et al., Performance of the LHCb RICH detector at the LHC, Eur. Phys. J. C 73 (2013) 2431, arXiv:1211.6759.
- [22] A.A. Alves Jr., et al., Performance of the LHCb muon system, J. Instrum. 8 (2013) P02022, arXiv:1211.1346.
- [23] T. Sjöstrand, S. Mrenna, P. Skands, PYTHIA 6.4 physics and manual, J. High Energy Phys. 0605 (2006) 026, arXiv:hep-ph/0603175.
- [24] T. Sjöstrand, S. Mrenna, P. Skands, A brief introduction to PYTHIA 8.1, Comput. Phys. Commun. 178 (2008) 852, arXiv:0710.3820.
- [25] I. Belyaev, et al., Handling of the generation of primary events in Gauss, the LHCb simulation framework, in: Nuclear Science Symposium Conference Record (NSS/MIC), 2010 IEEE, 2010, p. 1155.
- [26] D.J. Lange, The EvtGen particle decay simulation package, Nucl. Instrum. Methods A 462 (2001) 152.
- [27] P. Golonka, Z. Was, PHOTOS Monte Carlo: a precision tool for QED corrections in Z and W decays, Eur. Phys. J. C 45 (2006) 97, arXiv:hep-ph/0506026.
- [28] I. Balakireva, D. Melikhov, N. Nikitin, D. Tlisov, Forward-backward and CP-violating asymmetries in rare $B_{d,s} \rightarrow (\phi, \gamma)l^+l^-$ decays, Phys. Rev. D 81 (2010) 054024, arXiv:0911.0605.
- [29] A. Popov, N. Nikitin, D. Savrina, The EvtGen-based model for the Monte-Carlo generation of the rare radiative leptonic B-decays, PoS QFTHEP2010 (2010) 035.
- [30] Geant4 Collaboration, J. Allison, et al., Geant4 developments and applications, IEEE Trans. Nucl. Sci. 53 (2006) 270.
- [31] Geant4 Collaboration, S. Agostinelli, et al., Geant4: a simulation toolkit, Nucl. Instrum. Methods A 506 (2003) 250.
- [32] M. Clemencic, et al., The LHCb simulation application, GAUSS: design, evolution and experience, J. Phys. Conf. Ser. 331 (2011) 032023.
- [33] R. Aaij, et al., The LHCb trigger and its performance in 2011, J. Instrum. 8 (2013) P04022, arXiv:1211.3055.
- [34] V.V. Gligorov, M. Williams, Efficient, reliable and fast high-level triggering using a bonsai boosted decision tree, J. Instrum. 8 (2013) 2013P, arXiv:1210.6861.
- [35] LHCb Collaboration, R. Aaij, et al., Observation of a resonance in $B^+ \rightarrow K^+\mu^+\mu^-$ decays at low recoil, Phys. Rev. Lett. 111 (2013) 112003, arXiv:1307.7595.
- [36] L. Breiman, J.H. Friedman, R.A. Olshen, C.J. Stone, Classification and regression trees, Wadsworth international group, Belmont, California, USA, 1984.
- [37] R.E. Schapire, Y. Freund, A decision-theoretic generalization of on-line learning and an application to boosting, J. Comput. Syst. Sci. 55 (1997) 119.
- [38] G. Punzi, Sensitivity of searches for new signals and its optimization, in: L. Lyons, R. Mount, R. Reitmeyer (Eds.), Statistical Problems in Particle Physics, Astrophysics, and Cosmology, 2003, p. 79, arXiv:physics/0308063.
- [39] K. De Bruyn, et al., Branching ratio measurements of B_s^0 decays, Phys. Rev. D 86 (2012) 014027, arXiv:1204.1735.
- [40] LHCb Collaboration, R. Aaij, et al., Measurement of the fragmentation fraction ratio f_s/f_d and its dependence on B meson kinematics, J. High Energy Phys. 1304 (2013) 001, arXiv:1301.5286, f_s/f_d value updated in LHCb-CONF-2013-011.
- [41] ARGUS Collaboration, H. Albrecht, et al., Search for $b \rightarrow sy$ in exclusive decays of B mesons, Phys. Lett. B 229 (3) (1989) 304.
- [42] LHCb Collaboration, R. Aaij, et al., Measurement of the polarization amplitudes in $B^0 \rightarrow J/\psi K^*(892)^0$ decays, Phys. Rev. D 88 (2013) 052002, arXiv:1307.2782.
- [43] S.S. Wilks, The large-sample distribution of the likelihood ratio for testing composite hypotheses, Ann. Math. Stat. 9 (1938) 60.
- [44] M. Pivk, F.R. Le, Diberder, sPlot: a statistical tool to unfold data distributions, Nucl. Instrum. Methods A 555 (2005) 356, arXiv:physics/0402083.
- [45] BaBar Collaboration, B. Aubert, et al., Evidence for the $B^0 \rightarrow p\bar{p}K^*(892)^0$ and $B^+ \rightarrow \eta_c K^*(892)^+$ decays and study of the decay dynamics of B meson decays into $p\bar{p}h$ final states, Phys. Rev. D 76 (2007) 092004, arXiv:0707.1648.
- [46] Belle Collaboration, K. Abe, et al., Measurements of branching fractions and decay amplitudes in $B^0 \rightarrow J/\psi K^*(892)^0$ decays, Phys. Lett. B 538 (2002) 11, arXiv:hep-ex/0205021.
- [47] CLEO Collaboration, C. Jessop, et al., Measurement of the decay amplitudes and branching fractions of $B^0 \rightarrow J/\psi K^*(892)^0$ and $B^+ \rightarrow J/\psi K^+$ decays, Phys. Rev. Lett. 79 (1997) 4533, arXiv:hep-ex/9702013.

LHCb Collaboration

R. Aaij⁴¹, B. Adeva³⁷, M. Adinolfi⁴⁶, A. Affolder⁵², Z. Ajaltouni⁵, S. Akar⁶, J. Albrecht⁹, F. Alessio³⁸, M. Alexander⁵¹, S. Ali⁴¹, G. Alkhazov³⁰, P. Alvarez Cartelle³⁷, A.A. Alves Jr^{25,38}, S. Amato², S. Amerio²², Y. Amhis⁷, L. An³, L. Anderlini^{17,g}, J. Anderson⁴⁰, R. Andreassen⁵⁷, M. Andreotti^{16,f}, J.E. Andrews⁵⁸, R.B. Appleby⁵⁴, O. Aquines Gutierrez¹⁰, F. Archilli³⁸, A. Artamonov³⁵, M. Artuso⁵⁹, E. Aslanides⁶, G. Auremma^{25,n}, M. Baalouch⁵, S. Bachmann¹¹, J.J. Back⁴⁸, A. Badalov³⁶, C. Baesso⁶⁰, W. Baldini¹⁶, R.J. Barlow⁵⁴, C. Barschel³⁸, S. Barsuk⁷, W. Barter⁴⁷, V. Batozskaya²⁸, V. Battista³⁹, A. Bay³⁹, L. Beaucourt⁴, J. Beddow⁵¹, F. Bedeschi²³, I. Bediaga¹, S. Belogurov³¹, K. Belous³⁵, I. Belyaev³¹, E. Ben-Haim⁸, G. Bencivenni¹⁸, S. Benson³⁸, J. Benton⁴⁶, A. Berezhnoy³², R. Bernet⁴⁰, A. Bertolin²², M.-O. Bettler⁴⁷, M. van Beuzekom⁴¹, A. Bien¹¹, S. Bifani⁴⁵, T. Bird⁵⁴, A. Bizzeti^{17,i}, P.M. Bjørnstad⁵⁴, T. Blake⁴⁸, F. Blanc³⁹, J. Blouw¹⁰, S. Blusk⁵⁹, V. Bocci²⁵, A. Bondar³⁴, N. Bondar^{30,38}, W. Bonivento¹⁵, S. Borghi⁵⁴, A. Borgia⁵⁹, M. Borsato⁷, T.J.V. Bowcock⁵², E. Bowen⁴⁰, C. Bozzi¹⁶, D. Brett⁵⁴, M. Britsch¹⁰, T. Britton⁵⁹, J. Brodzicka⁵⁴, N.H. Brook⁴⁶, A. Bursche⁴⁰, J. Buytaert³⁸, S. Cadeddu¹⁵, R. Calabrese^{16,f}, M. Calvi^{20,k}, M. Calvo Gomez^{36,p}, P. Campana¹⁸, D. Campora Perez³⁸, L. Capriotti⁵⁴, A. Carbone^{14,d}, G. Carboni^{24,l}, R. Cardinale^{19,38,j}, A. Cardini¹⁵, L. Carson⁵⁰, K. Carvalho Akiba^{2,38}, R.C.M. Casanova Mohr³⁶, G. Casse⁵², L. Cassina^{20,k}, L. Castillo Garcia³⁸, M. Cattaneo³⁸, Ch. Cauet⁹, R. Cenci^{23,t}, M. Charles⁸, Ph. Charpentier³⁸, M. Chefdeville⁴, S. Chen⁵⁴, S.-F. Cheung⁵⁵, N. Chiapolini⁴⁰, M. Chrzaszcz^{40,26}, X. Cid Vidal³⁸, G. Ciezarek⁴¹, P.E.L. Clarke⁵⁰, M. Clemencic³⁸, H.V. Cliff⁴⁷, J. Closier³⁸, V. Coco³⁸, J. Cogan⁶, E. Cogneras⁵, V. Cogoni^{15,e}, L. Cojocariu²⁹, G. Collazuol²², P. Collins³⁸, A. Comerma-Montells¹¹, A. Contu^{15,38}, A. Cook⁴⁶, M. Coombes⁴⁶, S. Coquereau⁸, G. Corti³⁸, M. Corvo^{16,f}, I. Counts⁵⁶, B. Couturier³⁸, G.A. Cowan⁵⁰, D.C. Craik⁴⁸, A.C. Crocombe⁴⁸, M. Cruz Torres⁶⁰, S. Cunliffe⁵³, R. Currie⁵³, C. D'Ambrosio³⁸, J. Dalseno⁴⁶, P. David⁸, P.N.Y. David⁴¹, A. Davis⁵⁷, K. De Bruyn⁴¹, S. De Capua⁵⁴, M. De Cian¹¹, J.M. De Miranda¹, L. De Paula², W. De Silva⁵⁷, P. De Simone¹⁸, C.-T. Dean⁵¹, D. Decamp⁴, M. Deckenhoff⁹, L. Del Buono⁸, N. Déléage⁴, D. Derkach⁵⁵, O. Deschamps⁵, F. Dettori³⁸, B. Dey⁴⁰, A. Di Canto³⁸, A. Di Domenico²⁵, H. Dijkstra³⁸, S. Donleavy⁵², F. Dordei¹¹, M. Dorigo^{39,*}, A. Dosil Suárez³⁷, D. Dossett⁴⁸, A. Dovbnya⁴³, K. Dreimanis⁵², G. Dujany⁵⁴, F. Dupertuis³⁹, P. Durante³⁸, R. Dzhelyadin³⁵, A. Dziurda²⁶, A. Dzyuba³⁰, S. Easo^{49,38}, U. Egede⁵³, V. Egorychev³¹, S. Eidelman³⁴, S. Eisenhardt⁵⁰, U. Eitschberger⁹, R. Ekelhof⁹, L. Eklund⁵¹, I. El Rifai⁵, Ch. Elsasser⁴⁰, S. Ely⁵⁹, S. Esen¹¹, H.M. Evans⁴⁷, T. Evans⁵⁵, A. Falabella¹⁴, C. Färber¹¹, C. Farinelli⁴¹, N. Farley⁴⁵, S. Farry⁵², R. Fay⁵², D. Ferguson⁵⁰, V. Fernandez Albor³⁷, F. Ferreira Rodrigues¹, M. Ferro-Luzzi³⁸, S. Filippov³³, M. Fiore^{16,f}, M. Fiorini^{16,f}, M. Firlej²⁷, C. Fitzpatrick³⁹, T. Fiutowski²⁷, P. Fol⁵³, M. Fontana¹⁰, F. Fontanelli^{19,j}, R. Forty³⁸, O. Francisco², M. Frank³⁸, C. Frei³⁸, M. Frosini¹⁷, J. Fu^{21,38}, E. Furfaro^{24,l}, A. Gallas Torreira³⁷, D. Galli^{14,d}, S. Gallorini^{22,38}, S. Gambetta^{19,j}, M. Gandelman², P. Gandini⁵⁹, Y. Gao³, J. García Pardiñas³⁷, J. Garofoli⁵⁹, J. Garra Tico⁴⁷, L. Garrido³⁶, D. Gascon³⁶, C. Gaspar³⁸, U. Gastaldi¹⁶, R. Gauld⁵⁵, L. Gavardi⁹, G. Gazzoni⁵, A. Geraci^{21,v}, E. Gersabeck¹¹, M. Gersabeck⁵⁴, T. Gershon⁴⁸, Ph. Ghez⁴, A. Gianelle²², S. Gianì³⁹, V. Gibson⁴⁷, L. Giubega²⁹, V.V. Gligorov³⁸, C. Göbel⁶⁰, D. Golubkov³¹, A. Golutvin^{53,31,38}, A. Gomes^{1,a}, C. Gotti^{20,k}, M. Grabalosa Gándara⁵, R. Graciani Diaz³⁶, L.A. Granado Cardoso³⁸, E. Graugés³⁶, E. Graverini⁴⁰, G. Graziani¹⁷, A. Greco²⁹, E. Greening⁵⁵, S. Gregson⁴⁷, P. Griffith⁴⁵, L. Grillo¹¹, O. Grünberg⁶³, B. Gui⁵⁹, E. Gushchin³³, Yu. Guz^{35,38}, T. Gys³⁸, C. Hadjivasiliou⁵⁹, G. Haefeli³⁹, C. Haen³⁸, S.C. Haines⁴⁷, S. Hall⁵³, B. Hamilton⁵⁸, T. Hampson⁴⁶, X. Han¹¹, S. Hansmann-Menzemer¹¹, N. Harnew⁵⁵, S.T. Harnew⁴⁶, J. Harrison⁵⁴, J. He³⁸, T. Head³⁹, V. Heijne⁴¹, K. Hennessy⁵², P. Henrard⁵, L. Henry⁸, J.A. Hernando Morata³⁷, E. van Herwijnen³⁸, M. Heß⁶³, A. Hicheur², D. Hill⁵⁵, M. Hoballah⁵, C. Hombach⁵⁴, W. Hulsbergen⁴¹, N. Hussain⁵⁵, D. Hutchcroft⁵², D. Hynds⁵¹, M. Idzik²⁷, P. Ilten⁵⁶, R. Jacobsson³⁸, A. Jaeger¹¹, J. Jalocha⁵⁵, E. Jans⁴¹, A. Jawahery⁵⁸, F. Jing³, M. John⁵⁵, D. Johnson³⁸, C.R. Jones⁴⁷, C. Joram³⁸, B. Jost³⁸, N. Jurik⁵⁹, S. Kandybei⁴³, W. Kanso⁶, M. Karacson³⁸, T.M. Karbach³⁸, S. Karodia⁵¹, M. Kelsey⁵⁹, I.R. Kenyon⁴⁵, T. Ketel⁴², B. Khanji^{20,38,k}, C. Khurewathanakul³⁹, S. Klaver⁵⁴, K. Klimaszewski²⁸, O. Kochebina⁷, M. Kolpin¹¹, I. Komarov³⁹, R.F. Koopman⁴², P. Koppenburg^{41,38}, M. Korolev³², L. Kravchuk³³, K. Kreplin¹¹, M. Kreps⁴⁸, G. Krocker¹¹, P. Krokovny³⁴, F. Kruse⁹, W. Kucewicz^{26,o}, M. Kucharczyk^{20,26,k}, V. Kudryavtsev³⁴, K. Kurek²⁸, T. Kvaratskheliya³¹, V.N. La Thi³⁹, D. Lacarrere³⁸, G. Lafferty⁵⁴, A. Lai¹⁵, D. Lambert⁵⁰, R.W. Lambert⁴², G. Lanfranchi¹⁸, C. Langenbruch⁴⁸, B. Langhans³⁸, T. Latham⁴⁸, C. Lazzeroni⁴⁵, R. Le Gac⁶, J. van Leerdam⁴¹, J.-P. Lees⁴, R. Lefèvre⁵,

A. Leflat³², J. Lefrançois⁷, O. Leroy⁶, T. Lesiak²⁶, B. Leverington¹¹, Y. Li³, T. Likhomanenko⁶⁴, M. Liles⁵²,
 R. Lindner³⁸, C. Linn³⁸, F. Lionetto⁴⁰, B. Liu¹⁵, S. Lohn³⁸, I. Longstaff⁵¹, J.H. Lopes², P. Lowdon⁴⁰,
 D. Lucchesi^{22,r}, H. Luo⁵⁰, A. Lupato²², E. Luppi^{16,f}, O. Lupton⁵⁵, F. Machefert⁷, I.V. Machikhiliyan³¹,
 F. Maciuc²⁹, O. Maev³⁰, S. Malde⁵⁵, A. Malinin⁶⁴, G. Manca^{15,e}, G. Mancinelli⁶, A. Mapelli³⁸,
 J. Maratas⁵, J.F. Marchand⁴, U. Marconi¹⁴, C. Marin Benito³⁶, P. Marino^{23,t}, R. Märki³⁹, J. Marks¹¹,
 G. Martellotti²⁵, M. Martinelli³⁹, D. Martinez Santos⁴², F. Martinez Vidal⁶⁵, D. Martins Tostes²,
 A. Massafferri¹, R. Matev³⁸, Z. Mathe³⁸, C. Matteuzzi²⁰, A. Mazurov⁴⁵, M. McCann⁵³, J. McCarthy⁴⁵,
 A. McNab⁵⁴, R. McNulty¹², B. McSkelly⁵², B. Meadows⁵⁷, F. Meier⁹, M. Meissner¹¹, M. Merk⁴¹,
 D.A. Milanes⁶², M.-N. Minard⁴, N. Moggi¹⁴, J. Molina Rodriguez⁶⁰, S. Monteil⁵, M. Morandin²²,
 P. Morawski²⁷, A. Mordà⁶, M.J. Morello^{23,t}, J. Moron²⁷, A.-B. Morris⁵⁰, R. Mountain⁵⁹, F. Muheim⁵⁰,
 K. Müller⁴⁰, M. Mussini¹⁴, B. Muster³⁹, P. Naik⁴⁶, T. Nakada³⁹, R. Nandakumar⁴⁹, I. Nasteva²,
 M. Needham⁵⁰, N. Neri²¹, S. Neubert³⁸, N. Neufeld³⁸, M. Neuner¹¹, A.D. Nguyen³⁹, T.D. Nguyen³⁹,
 C. Nguyen-Mau^{39,q}, M. Nicol⁷, V. Niess⁵, R. Niet⁹, N. Nikitin³², T. Nikodem¹¹, A. Novoselov³⁵,
 D.P. O'Hanlon⁴⁸, A. Oblakowska-Mucha²⁷, V. Obraztsov³⁵, S. Ogilvy⁵¹, O. Okhrimenko⁴⁴,
 R. Oldeman^{15,e}, C.J.G. Onderwater⁶⁶, M. Orlandea²⁹, B. Osorio Rodrigues¹, J.M. Otalora Goicochea²,
 A. Otto³⁸, P. Owen⁵³, A. Oyanguren⁶⁵, B.K. Pal⁵⁹, A. Palano^{13,c}, F. Palombo^{21,u}, M. Palutan¹⁸,
 J. Panman³⁸, A. Papanestis^{49,38}, M. Pappagallo⁵¹, L.L. Pappalardo^{16,f}, C. Parkes⁵⁴, C.J. Parkinson^{9,45},
 G. Passaleva¹⁷, G.D. Patel⁵², M. Patel⁵³, C. Patrignani^{19,j}, A. Pearce^{54,49}, A. Pellegrino⁴¹, G. Penso^{25,m},
 M. Pepe Altarelli³⁸, S. Perazzini^{14,d}, P. Perret⁵, L. Pescatore⁴⁵, E. Pesen⁶⁷, K. Petridis⁵³, A. Petrolini^{19,j},
 E. Picatoste Olloqui³⁶, B. Pietrzyk⁴, T. Pilař⁴⁸, D. Pinci²⁵, A. Pistone¹⁹, S. Playfer⁵⁰, M. Plo Casasus³⁷,
 F. Polci⁸, A. Poluektov^{48,34}, I. Polyakov³¹, E. Polcarpo², A. Popov³⁵, D. Popov¹⁰, B. Popovici²⁹,
 C. Potterat², E. Price⁴⁶, J.D. Price⁵², J. Prisciandaro³⁹, A. Pritchard⁵², C. Prouve⁴⁶, V. Pugatch⁴⁴,
 A. Puig Navarro³⁹, G. Punzi^{23,s}, W. Qian⁴, B. Rachwal²⁶, J.H. Rademacker⁴⁶, B. Rakotomiaramanana³⁹,
 M. Rama²³, M.S. Rangel², I. Raniuk⁴³, N. Rauschmayr³⁸, G. Raven⁴², F. Redi⁵³, S. Reichert⁵⁴,
 M.M. Reid⁴⁸, A.C. dos Reis¹, S. Ricciardi⁴⁹, S. Richards⁴⁶, M. Rihl³⁸, K. Rinnert⁵², V. Rives Molina³⁶,
 P. Robbe⁷, A.B. Rodrigues¹, E. Rodrigues⁵⁴, P. Rodriguez Perez⁵⁴, S. Roiser³⁸, V. Romanovsky³⁵,
 A. Romero Vidal³⁷, M. Rotondo²², J. Rouvinet³⁹, T. Ruf³⁸, H. Ruiz³⁶, P. Ruiz Valls⁶⁵, J.J. Saborido Silva³⁷,
 N. Sagidova³⁰, P. Sail⁵¹, B. Saitta^{15,e}, V. Salustino Guimaraes², C. Sanchez Mayordomo⁶⁵,
 B. Sanmartin Sedes³⁷, R. Santacesaria²⁵, C. Santamarina Rios³⁷, E. Santovetti^{24,l}, A. Sarti^{18,m},
 C. Satriano^{25,n}, A. Satta²⁴, D.M. Saunders⁴⁶, D. Savrina^{31,32}, M. Schiller³⁸, H. Schindler³⁸, M. Schlupp⁹,
 M. Schmelling¹⁰, B. Schmidt³⁸, O. Schneider³⁹, A. Schopper³⁸, M.-H. Schune⁷, R. Schwemmer³⁸,
 B. Sciascia¹⁸, A. Sciubba^{25,m}, A. Semennikov³¹, I. Sepp⁵³, N. Serra⁴⁰, J. Serrano⁶, L. Sestini²²,
 P. Seyfert¹¹, M. Shapkin³⁵, I. Shapoval^{16,43,f}, Y. Shcheglov³⁰, T. Shears⁵², L. Shekhtman³⁴,
 V. Shevchenko⁶⁴, A. Shires⁹, R. Silva Coutinho⁴⁸, G. Simi²², M. Sirendi⁴⁷, N. Skidmore⁴⁶, I. Skillicorn⁵¹,
 T. Skwarnicki⁵⁹, N.A. Smith⁵², E. Smith^{55,49}, E. Smith⁵³, J. Smith⁴⁷, M. Smith⁵⁴, H. Snoek⁴¹,
 M.D. Sokoloff⁵⁷, F.J.P. Soler⁵¹, F. Soomro³⁹, D. Souza⁴⁶, B. Souza De Paula², B. Spaan⁹, P. Spradlin⁵¹,
 S. Sridharan³⁸, F. Stagni³⁸, M. Stahl¹¹, S. Stahl¹¹, O. Steinkamp⁴⁰, O. Stenyakin³⁵, F. Sterpka⁵⁹,
 S. Stevenson⁵⁵, S. Stoica²⁹, S. Stone⁵⁹, B. Storaci⁴⁰, S. Stracka^{23,t}, M. Straticiu²⁹, U. Straumann⁴⁰,
 R. Stroili²², L. Sun⁵⁷, W. Sutcliffe⁵³, K. Swientek²⁷, S. Swientek⁹, V. Syropoulos⁴², M. Szczekowski²⁸,
 P. Szczypka^{39,38}, T. Szumlak²⁷, S. T'Jampens⁴, M. Teklishyn⁷, G. Tellarini^{16,f}, F. Teubert³⁸, C. Thomas⁵⁵,
 E. Thomas³⁸, J. van Tilburg⁴¹, V. Tisserand⁴, M. Tobin³⁹, J. Todd⁵⁷, S. Tolk⁴², L. Tomassetti^{16,f},
 D. Tonelli³⁸, S. Topp-Joergensen⁵⁵, N. Torr⁵⁵, E. Tournefier⁴, S. Tourneur³⁹, M.T. Tran³⁹, M. Tresch⁴⁰,
 A. Trisovic³⁸, A. Tsaregorodtsev⁶, P. Tsopelas⁴¹, N. Tuning⁴¹, M. Ubeda Garcia³⁸, A. Ukleja²⁸,
 A. Ustyuzhanin⁶⁴, U. Uwer¹¹, C. Vacca^{15,e}, V. Vagnoni¹⁴, G. Valenti¹⁴, A. Vallier⁷, R. Vazquez Gomez¹⁸,
 P. Vazquez Regueiro³⁷, C. Vázquez Sierra³⁷, S. Vecchi¹⁶, J.J. Velthuis⁴⁶, M. Veltri^{17,h}, G. Veneziano³⁹,
 M. Vesterinen¹¹, J.V.V.B.Viana Barbosa³⁸, B. Viaud⁷, D. Vieira², M. Vieites Diaz³⁷,
 X. Vilasis-Cardona^{36,p}, A. Vollhardt⁴⁰, D. Volyanskyy¹⁰, D. Voong⁴⁶, A. Vorobyev³⁰, V. Vorobyev³⁴,
 C. Voß⁶³, J.A. de Vries⁴¹, R. Waldi⁶³, C. Wallace⁴⁸, R. Wallace¹², J. Walsh²³, S. Wandernoth¹¹,
 J. Wang⁵⁹, D.R. Ward⁴⁷, N.K. Watson⁴⁵, D. Websdale⁵³, M. Whitehead⁴⁸, D. Wiedner¹¹,
 G. Wilkinson^{55,38}, M. Wilkinson⁵⁹, M.P. Williams⁴⁵, M. Williams⁵⁶, H.W. Wilschut⁶⁶, F.F. Wilson⁴⁹,
 J. Wimberley⁵⁸, J. Wishahi⁹, W. Wislicki²⁸, M. Witek²⁶, G. Wormser⁷, S.A. Wotton⁴⁷, S. Wright⁴⁷,

K. Wyllie³⁸, Y. Xie⁶¹, Z. Xing⁵⁹, Z. Xu³⁹, Z. Yang³, X. Yuan³, O. Yushchenko³⁵, M. Zangoli¹⁴,
M. Zavertyaev^{10,b}, L. Zhang³, W.C. Zhang¹², Y. Zhang³, A. Zhelezov¹¹, A. Zhokhov³¹, L. Zhong³

- ¹ Centro Brasileiro de Pesquisas Físicas (CBPF), Rio de Janeiro, Brazil
² Universidade Federal do Rio de Janeiro (UFRJ), Rio de Janeiro, Brazil
³ Center for High Energy Physics, Tsinghua University, Beijing, China
⁴ LAPP, Université de Savoie, CNRS/IN2P3, Annecy-Le-Vieux, France
⁵ Clermont Université, Université Blaise Pascal, CNRS/IN2P3, LPC, Clermont-Ferrand, France
⁶ CPPM, Aix-Marseille Université, CNRS/IN2P3, Marseille, France
⁷ LAL, Université Paris-Sud, CNRS/IN2P3, Orsay, France
⁸ LPNHE, Université Pierre et Marie Curie, Université Paris Diderot, CNRS/IN2P3, Paris, France
⁹ Fakultät Physik, Technische Universität Dortmund, Dortmund, Germany
¹⁰ Max-Planck-Institut für Kernphysik (MPIK), Heidelberg, Germany
¹¹ Physikalisches Institut, Ruprecht-Karls-Universität Heidelberg, Heidelberg, Germany
¹² School of Physics, University College Dublin, Dublin, Ireland
¹³ Sezione INFN di Bari, Bari, Italy
¹⁴ Sezione INFN di Bologna, Bologna, Italy
¹⁵ Sezione INFN di Cagliari, Cagliari, Italy
¹⁶ Sezione INFN di Ferrara, Ferrara, Italy
¹⁷ Sezione INFN di Firenze, Firenze, Italy
¹⁸ Laboratori Nazionali dell'INFN di Frascati, Frascati, Italy
¹⁹ Sezione INFN di Genova, Genova, Italy
²⁰ Sezione INFN di Milano Bicocca, Milano, Italy
²¹ Sezione INFN di Milano, Milano, Italy
²² Sezione INFN di Padova, Padova, Italy
²³ Sezione INFN di Pisa, Pisa, Italy
²⁴ Sezione INFN di Roma Tor Vergata, Roma, Italy
²⁵ Sezione INFN di Roma La Sapienza, Roma, Italy
²⁶ Henryk Niewodniczanski Institute of Nuclear Physics Polish Academy of Sciences, Kraków, Poland
²⁷ AGH – University of Science and Technology, Faculty of Physics and Applied Computer Science, Kraków, Poland
²⁸ National Center for Nuclear Research (NCBJ), Warsaw, Poland
²⁹ Horia Hulubei National Institute of Physics and Nuclear Engineering, Bucharest-Magurele, Romania
³⁰ Petersburg Nuclear Physics Institute (PNPI), Gatchina, Russia
³¹ Institute of Theoretical and Experimental Physics (ITEP), Moscow, Russia
³² Institute of Nuclear Physics, Moscow State University (SINP MSU), Moscow, Russia
³³ Institute for Nuclear Research of the Russian Academy of Sciences (INR RAN), Moscow, Russia
³⁴ Budker Institute of Nuclear Physics (SB RAS) and Novosibirsk State University, Novosibirsk, Russia
³⁵ Institute for High Energy Physics (IHEP), Protvino, Russia
³⁶ Universitat de Barcelona, Barcelona, Spain
³⁷ Universidad de Santiago de Compostela, Santiago de Compostela, Spain
³⁸ European Organization for Nuclear Research (CERN), Geneva, Switzerland
³⁹ Ecole Polytechnique Fédérale de Lausanne (EPFL), Lausanne, Switzerland
⁴⁰ Physik-Institut, Universität Zürich, Zürich, Switzerland
⁴¹ Nikhef National Institute for Subatomic Physics, Amsterdam, The Netherlands
⁴² Nikhef National Institute for Subatomic Physics and VU University Amsterdam, Amsterdam, The Netherlands
⁴³ NSC Kharkiv Institute of Physics and Technology (NSC KIPT), Kharkiv, Ukraine
⁴⁴ Institute for Nuclear Research of the National Academy of Sciences (KINR), Kyiv, Ukraine
⁴⁵ University of Birmingham, Birmingham, United Kingdom
⁴⁶ H.H. Wills Physics Laboratory, University of Bristol, Bristol, United Kingdom
⁴⁷ Cavendish Laboratory, University of Cambridge, Cambridge, United Kingdom
⁴⁸ Department of Physics, University of Warwick, Coventry, United Kingdom
⁴⁹ STFC Rutherford Appleton Laboratory, Didcot, United Kingdom
⁵⁰ School of Physics and Astronomy, University of Edinburgh, Edinburgh, United Kingdom
⁵¹ School of Physics and Astronomy, University of Glasgow, Glasgow, United Kingdom
⁵² Oliver Lodge Laboratory, University of Liverpool, Liverpool, United Kingdom
⁵³ Imperial College London, London, United Kingdom
⁵⁴ School of Physics and Astronomy, University of Manchester, Manchester, United Kingdom
⁵⁵ Department of Physics, University of Oxford, Oxford, United Kingdom
⁵⁶ Massachusetts Institute of Technology, Cambridge, MA, United States
⁵⁷ University of Cincinnati, Cincinnati, OH, United States
⁵⁸ University of Maryland, College Park, MD, United States
⁵⁹ Syracuse University, Syracuse, NY, United States
⁶⁰ Pontifícia Universidade Católica do Rio de Janeiro (PUC-Rio), Rio de Janeiro, Brazil^w
⁶¹ Institute of Particle Physics, Central China Normal University, Wuhan, Hubei, China^x
⁶² Departamento de Física, Universidad Nacional de Colombia, Bogota, Colombia^y
⁶³ Institut für Physik, Universität Rostock, Rostock, Germany^z
⁶⁴ National Research Centre Kurchatov Institute, Moscow, Russia^{aa}
⁶⁵ Instituto de Física Corpuscular (IFIC), Universitat de Valencia-CSIC, Valencia, Spain^{ab}
⁶⁶ Van Swinderen Institute, University of Groningen, Groningen, The Netherlands^{ac}
⁶⁷ Celal Bayar University, Manisa, Turkey^{ad}

* Corresponding author.

E-mail address: mirco.dorigo@cern.ch (M. Dorigo).

^a Universidade Federal do Triângulo Mineiro (UFTM), Uberaba-MG, Brazil.

^b P.N. Lebedev Physical Institute, Russian Academy of Science (LPI RAS), Moscow, Russia.

^c Università di Bari, Bari, Italy.

^d Università di Bologna, Bologna, Italy.

- ^e Università di Cagliari, Cagliari, Italy.
- ^f Università di Ferrara, Ferrara, Italy.
- ^g Università di Firenze, Firenze, Italy.
- ^h Università di Urbino, Urbino, Italy.
- ⁱ Università di Modena e Reggio Emilia, Modena, Italy.
- ^j Università di Genova, Genova, Italy.
- ^k Università di Milano Bicocca, Milano, Italy.
- ^l Università di Roma Tor Vergata, Roma, Italy.
- ^m Università di Roma La Sapienza, Roma, Italy.
- ⁿ Università della Basilicata, Potenza, Italy.
- ^o AGH – University of Science and Technology, Faculty of Computer Science, Electronics and Telecommunications, Kraków, Poland.
- ^p LIFAELS, La Salle, Universitat Ramon Llull, Barcelona, Spain.
- ^q Hanoi University of Science, Hanoi, Viet Nam.
- ^r Università di Padova, Padova, Italy.
- ^s Università di Pisa, Pisa, Italy.
- ^t Scuola Normale Superiore, Pisa, Italy.
- ^u Università degli Studi di Milano, Milano, Italy.
- ^v Politecnico di Milano, Milano, Italy.
- ^w Associated to: Universidade Federal do Rio de Janeiro (UFRJ), Rio de Janeiro, Brazil.
- ^x Associated to: Center for High Energy Physics, Tsinghua University, Beijing, China.
- ^y Associated to: LPNHE, Université Pierre et Marie Curie, Université Paris Diderot, CNRS/IN2P3, Paris, France.
- ^z Associated to: Physikalisches Institut, Ruprecht-Karls-Universität Heidelberg, Heidelberg, Germany.
- ^{aa} Associated to: Institute of Theoretical and Experimental Physics (ITEP), Moscow, Russia.
- ^{ab} Associated to: Universitat de Barcelona, Barcelona, Spain.
- ^{ac} Associated to: Nikhef National Institute for Subatomic Physics, Amsterdam, The Netherlands.
- ^{ad} Associated to: European Organization for Nuclear Research (CERN), Geneva, Switzerland.